European Journal of Radiology Open 8 (2021) 100362

Contents lists available at ScienceDirect

European Journal of Radiology Open

journal homepage: www.elsevier.com/locate/ejro

Quantitative volumetry of ground-glass nodules on high-spatial-resolution CT with 0.25-mm section thickness and 1024 matrix: Phantom and clinical studies

Yuriko Yoshida [a], Masahiro Yanagawa [a,*], Akinori Hata [a], Yukihisa Sato [b], Mitsuko Tsubamoto [c], Shuhei Doi [a], Kazuki Yamagata [a], Tomo Miyata [d], Noriko Kikuchi [a], Noriyuki Tomiyama [a]

[a] Department of Diagnostic and Interventional Radiology, Osaka University Graduate School of Medicine, 2-2 Yamadaoka Suita, Osaksa 565-0871, Japan
[b] Department of Diagnostic Radiology, Suita Municipal Hospital, 5-7 Kishibeshinmachi Suita, Osaka 564-8567, Japan
[c] Department of Diagnositic Radiology, Nishinomiya Municipal Central Hospital, 8-24 Hayashidacho, Nishinomiya, Hyogo, 663-8014, Japan
[d] Department of Future Diagnostic Radiology, Osaka University Graduate School of Medicine 2-2 Yamadaoka Suita, Osaksa 565-0871, Japan

HIGHLIGHTS

- High-spatial-resolution CT provided more accurate volume of a −800-HU nodule in a phantom than conventional settings.
- The maximum CT attenuation values were significantly higher in high-resolution setting than conventional setting.
- The high-resolution setting might allow earlier detection of solid components in GGNs during follow-up.

ARTICLE INFO

Keywords:
Solitary pulmonary nodule
Lung
Spiral computed tomography

ABSTRACT

Objectives: To compare high-resolution (HR) and conventional (C) settings of high-spatial-resolution computed tomography (CT) for software volumetry of ground-glass nodules (GGNs) in phantoms and patients.
Methods: We placed −800 and −630 HU spherical GGN-mimic nodules in 28 different positions in phantoms and scanned them individually. Additionally, 60 GGNs in 45 patients were assessed retrospectively. Images were reconstructed using the HR-setting (matrix size, 1024; slice thickness, 0.25 mm) and C-setting (matrix size, 512; slice thickness, 0.5 mm). We measured the GGN volume and mass using software. In the phantom study, the absolute percentage error (APE) was calculated as the absolute difference between Vernier caliper measurement-based and software-based volumes. In patients, we measured the density (mean, maximum, and minimum) and classified GGNs into low- and high-attenuation GGNs.
Results: In images of the −800 HU, but not −630 HU, phantom nodules, the volumes and masses differed significantly between the two settings (both $p < 0.01$). The APE was significantly lower in the HR-setting than in the C-setting ($p < 0.01$). In patients, volumes did not differ significantly between settings ($p = 0.59$). Although the mean attenuation was not significantly different, the maximum and minimum values were significantly increased and decreased, respectively, in the HR-setting (both $p < 0.01$). The volumes of both low-attenuation and high-attenuation GGNs were not significantly different between settings ($p = 0.78$ and 0.39, respectively).
Conclusion: The HR-setting might yield a more accurate volume for phantom GGN of −800 HU and influence the detection of maximum and minimum CT attenuation.

1. Introduction

The possibility to detect ground-glass nodules (GGNs) is rapidly increasing due to recent advances in computed tomography (CT), its common use in clinical practice, and the introduction of this technology in mass screenings for early lung cancer. GGNs can be observed in both

Abbreviations: 3D, three-dimensional; APE, absolute percentage error; C-CT, conventional computed tomography; C-setting, conventional setting; CT, computed tomography; GGN, ground-glass nodule; HR-setting, high-resolution setting; HSR-CT, high-spatial-resolution computed tomography; VDT, volume doubling time.

* Corresponding author.
E-mail address: m-yanagawa@radiol.med.osaka-u.ac.jp (M. Yanagawa).

https://doi.org/10.1016/j.ejro.2021.100362
Received 11 April 2021; Received in revised form 26 May 2021; Accepted 29 May 2021
2352-0477/© 2021 The Author(s). Published by Elsevier Ltd. This is an open access article under the CC BY-NC-ND license (http://creativecommons.org/licenses/by-nc-nd/4.0/).

benign and malignant conditions, including adenocarcinoma *in situ* and its preinvasive lesion, atypical adenomatous hyperplasia [1]. GGNs have great clinical significance, because the prevalence of malignancy is higher in GGNs than in solid nodules [2]. Differentiating adenocarcinoma from other, benign conditions is very important for an accurate diagnosis and selecting optimal treatment.

The volume doubling time (VDT) is useful for the evaluation of the growth rate of persistent GGNs. Previous studies have shown that a shorter VDT in GGN may suggest greater histological tumor aggressiveness [3,4]. It has been recognized that computer-aided three-dimensional (3D) volume determination is more reliable than manual volume measurement [5]. However, a significantly increased error occurs in volume measurements of GGNs than in that of solid nodules, because the delineation of GGNs from the surrounding lung tissue is more difficult, even in computer-aided measurements, due to the decreased contrast [6].

Recent studies have reported that high-spatial-resolution CT (HSR-CT) can describe detailed structures and provide significantly higher image quality than conventional CT (C-CT) for the evaluation of abnormal CT findings, including ground-glass opacities [7]. HSR-CT can reconstruct images with higher quality when using a high-resolution setting (HR-setting), a slice thickness of 0.25 mm, and a large matrix size. To our knowledge, no previous study has attempted to quantify or predict the effects of volumetric GGN measurement using HSR-CT. We hypothesized that the HR-setting would allow more accurate volume measurements. Thus, this study aimed to assess the effects of using the HR-setting and conventional setting (C-setting) of HSR-CT on software volumetry, using images of GGNs in a phantom and in clinical patients.

2. Materials and methods

2.1. Phantom study

A torso phantom (N1 LUNGMAN, Kyoto Kagaku Co., Ltd.) was used for this study. A network of small structures adhering to the heart/mediastinum was designed to be similar to vascular and bronchial structures. The phantom does not have a medium that mimics the lung parenchyma and instead is filled with air. To simulate GGNs, we used one off-the-shelf artificial spherical nodule for each with attenuation values of −630 and −800 HU, respectively. We randomly attached each of two nodules individually to the phantom at 28 different locations and performed scans using both settings for each location.

The nominal diameter of both nodules was 10 mm, but to measure the volume more accurately, the diameter of each nodule was measured 100 times using a digital Vernier caliper (0.01 mm), and the assumed volume of each nodule was calculated from the average diameter, using the formula $V = 4/3 \times \pi r^3$ with r being the average radius.

2.2. Clinical study

This study was approved by the institutional ethics review board. The need to obtain informed consent for this retrospective review of patient records and images was waived. One chest radiologist with 4 years' experience reviewed the CT images of consecutive patients who underwent non-contrast-enhanced CT of the chest at a single institute from June through September 2018 and in whom GGNs were identified. We enrolled images of nodules that satisfied the following criteria: (1) the long axis, measured manually, was more than 6 mm, (2) there was no solid component, and (3) the CT raw data were available for retrospective reconstructions. Criterion (1) was based on the Guidelines for the Management of Incidental Pulmonary Nodules Detected on CT Images of the Fleischner Society, 2017 [8].

Sixty-five pure GGNs in 48 patients were enrolled. Because the software could not delineate five nodules in three patients, they were excluded. Finally, we assessed 60 nodules in 45 patients (male: 15, female, 30; age range, 26–87 years, mean age, 65.8 years; Fig. 1).

2.3. CT image acquisition

Both phantom and clinical images were obtained using an HSR-CT scanner (Aquilion Precision: Canon Medical Systems). The CT scanner had 160 detector rows with a 0.25-mm detector row-width and 1792 detector channels, supporting image reconstruction with a 1024 × 1024 matrix. The scanning protocol was as follows: tube voltage, 120 kVp; focus size, 0.6 × 0.6 mm; 0.5-ms gantry rotation time in spiral mode, and auto-exposure control. The clinical images were obtained during breath-hold at full inspiration, and the range of CT scans was the whole lung. CT images were reconstructed using both the HR-setting (matrix size, 1024 × 1024; slice thickness, 0.25 mm; field of view, 34.5 cm; FC 51 with adaptive iterative dose reduction) and the C-setting (matrix size, 512 × 512; slice thickness, 0.5 mm; field of view, 34.5 cm; FC 51 with adaptive iterative dose reduction) for both phantom and clinical data. According to the scanner report, the volumetric CT dose index was 13.5 mGy in the phantom study and 13.0 ± 1.0 mGy in the clinical study.

2.4. Image analysis

Commercially available, semi-automated software (Vitrea: Canon Medical Systems) was used to analyze the CT images. The investigator clicked on the nodule image, the software automatically delineated the nodule and measured the volume and density (mean, maximum, and minimum) within the nodule. The maximum and minimum referred to the highest and lowest CT values, respectively, among all voxel CT values constituting the nodule (Fig. 2). This software extracted a nodal region around a user-specified point using the threshold value calculated for each case by histogram analysis. Next, image features were calculated for each voxel in the nodal region. The features were used to

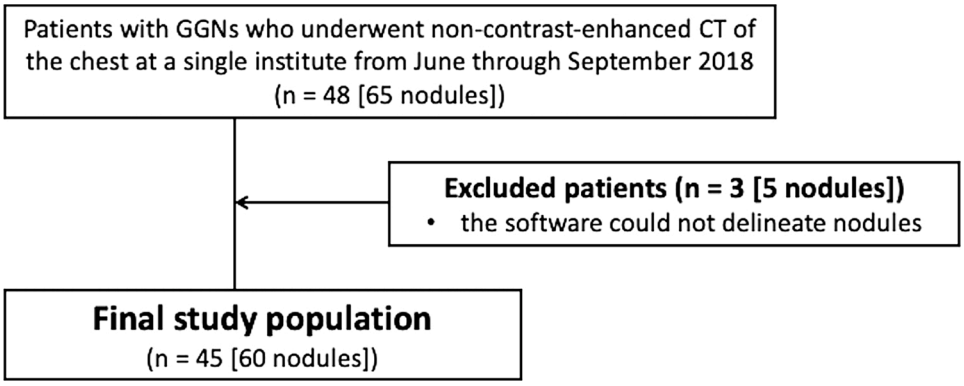

Fig. 1. Flowchart of patient selection and demographics.

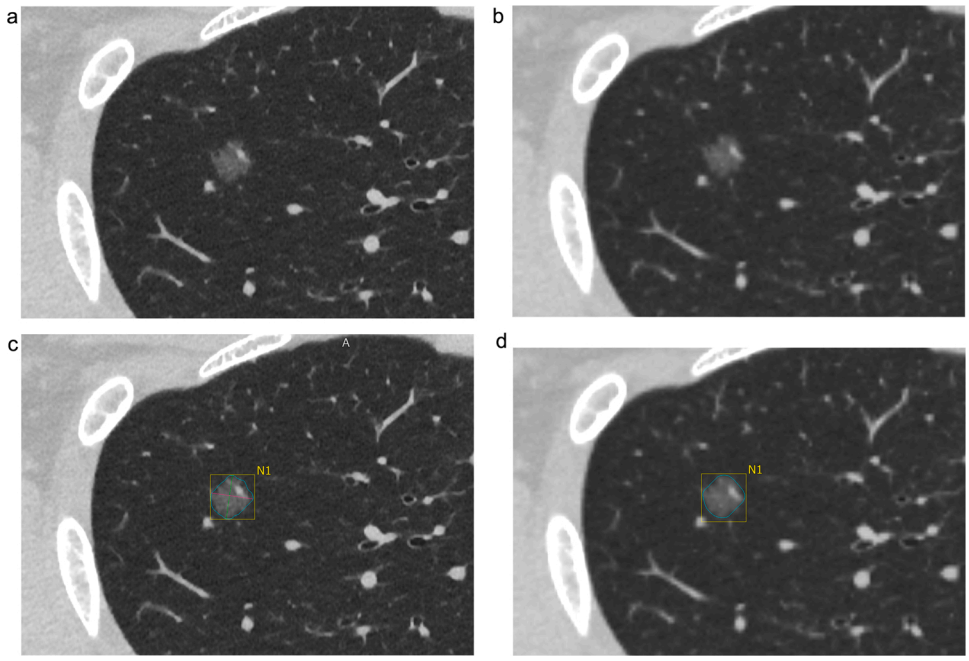

Fig. 2. Example of nodule volumetry in high-resolution setting (HR-setting) and conventional setting (C-setting) images in the clinical study. (a) Ground-glass nodule (GGN) in a HR-setting image. (b) GGN in a C-setting image. (c) The software automatically estimates the nodule border to calculate the nodule volume and attenuation in HR-setting images. A manual correction is not performed for this nodule. The volume is 339.1 mm^3. The average, maximum, and minimum attenuation values are −628 HU, 20 HU, and −963 HU, respectively. (d) The software also automatically determines nodule border, nodule volume, and attenuation in C-setting images. A manual correction is not performed for this nodule. The volume is 341.0 mm^3. The average, maximum, and minimum attenuation values are −628 HU, −74 HU, and −893 HU, respectively.

remove blood vessels from the nodal region. The volume was measured by counting the number of voxels contained in the remaining nodal region.

Using this software, two radiologists ([BLINDED FOR REVIEW] with 12 years' experience and [BLINDED FOR REVIEW] with 26 years' experience) independently and blinded to the setting measured the volumes of all nodules in the images obtained with either the HR-setting or the C-setting. In the clinical study, we also measured the mean, minimum, and maximum density of the GGNs with the software. Segmentation was considered successful when the nodule was almost completely delineated. If the segmentation was not successful, a manual correction was performed. It was visually confirmed by the investigator that the segmentation area covered the edge of the three-dimensional nodule.

2.5. Statistical analysis

To assess interobserver variability, the differences in the values obtained between the two radiologists were plotted against the respective means to obtain Bland-Altman plots, indicating the limits of agreements (95 % confidence intervals) between the observers, using MedCalc (version 19.2.1.; MedCalc Software, Ltd.) [9].

In the phantom study, we expressed the measured volume of the GGNs as absolute percentage error (APE), which was calculated using the following formula: $APE = (|V_{ass.}\text{-}V_{cal.}| / V_{ass.}) \times 100$ with $V_{ass.}$ indicating the assumed nodule volume calculated from the measurements using the digital Vernier caliper and $V_{cal.}$ the volume determined by volumetry on CT images. The average of the values obtained by the two radiologists was used as $V_{cal.}$ The Shpairo-Wilk test was performed to assess normality, and there was no normality in all data. The Wilcoxon signed-rank test was used to evaluate the difference between the two settings in terms of nodule volumetry results and APE values.

In the clinical study, we analyzed all nodules in both settings. Additionally, we classified GGNs into two groups based on CT value: low-attenuation GGNs and high-attenuation GGNs. The entire nodule was divided into two groups using the cutoff value of CT attenuation: low-attenuation GGNs below the cutoff value and high-attenuation GGNs above the cutoff value. The cutoff value of −700 HU was decided so that the mean value of all high-attenuation GGNs was about −630 HU to be comparable with the results of the higher density of the two phantom nodules (-630 HU). In this study, only one clinical case showed a CT attenuation of −800 HU or less in the C-setting. The Shpairo-Wilk test was performed to assess normality, and there was no normality in all data. The Wilcoxon signed-rank test was used to evaluate the differences in nodule volumetry and attenuation between the two settings.

In both studies, we evaluated the nodules using GGN mass values. Adding 1000 to the mean CT attenuation in HU translates this value into density in mg/cm^3, which can be multiplied by the GGN volume to yield the GGN mass [10,11]. In the phantom study, the CT attenuation values used in these calculations were −800 HU and −630 HU, and in the clinical study, the average CT attenuation of each nodule was used. Statistical analyses, except for Bland-Altman plots, were performed using JMP (version 14.0; SAS Institute Inc.). $P < 0.05$ indicated a statistically significant difference.

3. Results

3.1. Phantom study

The diameter of the -800HU nodule measured using the Vernier caliper was 10.1 mm, with an assumed volume of 544.8 mm^3, and the diameter of the -630HU nodule was 10.0 mm, with an assumed volume of 515.9 mm^3. Table 1 shows the APE values and measured volumes. For the −630-HU nodule, the APE, volume, and GGN mass were not significantly different between the two settings ($p = 0.85$, 0.65, and 0.65, respectively). For the −800 HU nodule, all APE, volume, and GGN mass values were significantly lower on HR-setting images than on C-setting images (all $p < 0.01$). No manual corrections were necessary in the phantom study. The determined volume of 544.8 mm^3 for the −800 HU nodule was close to the measured volume of 577.0 mm^3 on CT image using the HR-setting.

3.2. Clinical study

Data for all nodules in the clinical study are presented in Table 2. There were no significant differences in volume, GGN mass, and mean CT attenuation between the HR-setting and the C-setting ($p = 0.59$, 0.57, and 0.15 respectively). However, there were significant differences between these settings regarding maximum and minimum CT attenuation

Table 1
Volume, absolute percentage error, and GGN mass in the artificial nodules with different attenuation.

	−800 HU			−630 HU		
	HR-setting	C-setting	p	HR-setting	C-setting	p
Volume (mm^3)	577.0 (563.0, 582.8)	583.9 (573.1, 595.1)	<0.01*	488.3 (480.7, 492.8)	488,8 (482.4, 497.4)	0.65
APE (%)	6.00 (4.24, 7.07)	7.56 (5.74, 9.45)	<0.01*	5.34 (3.09, 6.82)	5.25 (3.57, 6.48)	0.85
GGN mass (mg)	115.4 (112.6, 116.6)	116.8 (114.6, 119.0)	<0.01*	180.7 (177.8, 182.3)	180.8 (178.5, 184.0)	0.65

The median and quartiles (first and third quartiles) of the artificial nodules are shown for volume, APE, and GGN mass.
* Significantly different in the Wilcoxon signed-rank test.
APE, absolute percentage error; *C-setting*, conventional setting; *GGN*, ground-glass nodule; *HR-setting*, high-resolution setting.

Table 2
Volume, GGN mass, and CT attenuation (mean, minimum, and maximum) in the clinical GGN samples.

n = 60	HR-setting	C-setting	p
Volume (mm^3)	187.3 (118.4, 397.7)	207.7 (131.0, 375.4)	0.59
GGN mass (mg)	65.0 (37.0, 145.6)	67.2 (37.9, 148.6)	0.57
CT attenuation (HU)			
Mean[a]	−676.3 (−714.6, −611.4)	−680.8 (−716.8, −622.0)	0.15
Min[b]	−954.3 (−995.9, −928.0)	−893.5 (−931.9, −860.1)	<0.01*
Max[c]	−62.8 (−271.3, 18.9)	−182.5 (−383.8, −74.3)	<0.01*

The median and quartiles (first and third quartiles) of clinical GGNs are shown for volume, GGN mass, and CT attenuation.
* Significantly different in the Wilcoxon signed-rank test.
[a] Using the mean CT value within each nodule, the median and quartiles (first and third quartiles) of 60 nodules is calculated.
[b] Using the min within each nodule, the median and quartiles (first and third quartiles) of 60 nodules is calculated. Min means the lowest CT value among all voxel CT values constituting the nodule.
[c] Using the max within each nodule, the median and quartiles (first and third quartiles) of 60 nodules is calculated. Max means the highest CT value among all voxel CT values constituting the nodule.
C-setting, conventional setting; *GGN*, ground-glass nodule; *HR-setting*, high-resolution setting.

(both $p < 0.01$). Table 3 shows the results of the subgroup analysis in which the nodules were classified into low-attenuation GGNs and high-attenuation GGNs. There were also no significant differences in volume and GGN mass when GGNs were grouped by CT attenuation. There were significant differences in maximum and minimum CT attenuation (both $p < 0.01$), but no significant difference in mean attenuation ($p = 0.15$).

3.3. Measurement variability

Bland-Altman plots are shown in Figs. 3 and 4. In the phantom study, there was no significant bias between the two observers in the measured volumes of the −800 HU and −630 HU nodules in either the high-definition or conventional settings (HR-setting, −800 HU, $p = 0.33$; C-setting, −800 HU, $p = 0.33$; HR-setting, −630 HU, $p = 0.29$; and C-setting, −630 HU, $p = 0.33$) (Fig. 3). In the clinical study, there were also no significant differences between observers regarding the measured volumes (HR-setting, $p = 0.54$; C-setting, $p = 0.11$) and GGN mass (HR-setting, $p = 0.46$; C-setting, $p = 0.32$) (Fig. 4).

4. Discussion

This study showed that the measured volume of the −800 HU nodule was significantly smaller in the HR-setting than in the C-setting, and that in the phantom study, the HR-setting improved the accuracy of the volumetric measurement of the −800 HU nodule, compared to the C-setting. On the other hand, there were no differences in the measured volume of the −630 HU nodule between the HR-setting and C-setting. In clinical cases, the measured volume and GGN mass did not significantly differ between the two settings. When GGNs were divided into two groups by CT attenuation with a threshold of −700 HU, the results of the clinical high-attenuation GGNs (mean attenuation, about −630 HU) were consistent with those of the artificial nodule with −630 HU. Low-attenuation GGNs (mean attenuation, about −740 HU) did not show significant differences in the clinical study. Some publications reported on the image quality in the HSR-CT, but to the best of our knowledge, no previous study evaluated volumetric measurements using HSR-CT.

In our phantom study, the HR-setting was advantageous for nodule volumetry. The partial volume effect adversely affects volumetric measurements and depends on reconstruction parameters, such as slice thickness and matrix size. A previous study reported a 20 % difference in volumetric tumor measurements between low (2–3 mm) and high (8–10 mm) slice-thickness settings [12]. On HR-setting images with a low slice-thickness and a large matrix size, the voxel size is smaller. We assume that decreasing the voxel size reduced the influence of partial volume effects and improved the accuracy of volume measurements. Most volumetry software packages, including the one we used, use the voxel-counting method to measure the volume of a nodule [5].

Table 3
Volume, GGN mass, and attenuation (mean, minimum, and maximum) for low- and high-attenuation GGNs.

	Low-attenuation GGNs (n = 20)			High-attenuation GGNs (n = 40)		
	HR-setting	C-setting	p	HR-setting	C-setting	p
Volume (mm^3)	166.5 (117.0, 359.1)	189.0 (127.3, 375.4)	0.55	229.4 (120.2, 464.8)	233.6 (139.5, 423.9)	0.37
GGN mass (mg)	43.8 (30.2, 97.6)	46.2 (30.7, 100.8)	0.78	82.7 (43.0, 167.4)	79.9 (48.9, 169.0)	0.39
CT attenuation (HU)						
Mean[a]	−733.5 (−753.6, −713.9)	−733.0 (−735.1, −712.3)	0.84	−640.5 (−676.4, -582.6)	−638.3 (−680.9, −593.1)	0.15
Min[b]	−974.0 (−933.9, −937.0)	−896.5 (−938.1, −860.5)	<0.01*	−947.8 (−1001.8, −921.9)	−891.5 (−929.0, −862.1)	<0.01*
Max[c]	−146.5 (−358.0, 0.6)	−367.0 (−502.3, −132.8	<0.01*	−42 (−189.3, 52.3)	−153.5 (−272.3, −30.5)	<0.01*

The median and quartiles (first and third quartiles) of 20 low-attenuation GGNs and 40 high-attenuation GGNs are shown for volume, GGN mass, and CT attenuation.
* Significantly different in the Wilcoxon signed-rank test.
[a] Using the mean CT value within each nodule, the median and quartiles (first and third quartiles) was calculated.
[b] Using the min within each nodule, the median and quartiles (first and third quartiles) was calculated. Min means the lowest CT value among all voxel CT values constituting the nodule.
[c] Using the max within each nodule, the median and quartiles (first and third quartiles) was calculated. Max means the highest CT value among all voxel CT values constituting the nodule.
C-setting, conventional setting; *GGN*, ground-glass nodule; *HR-setting*, high-resolution setting.

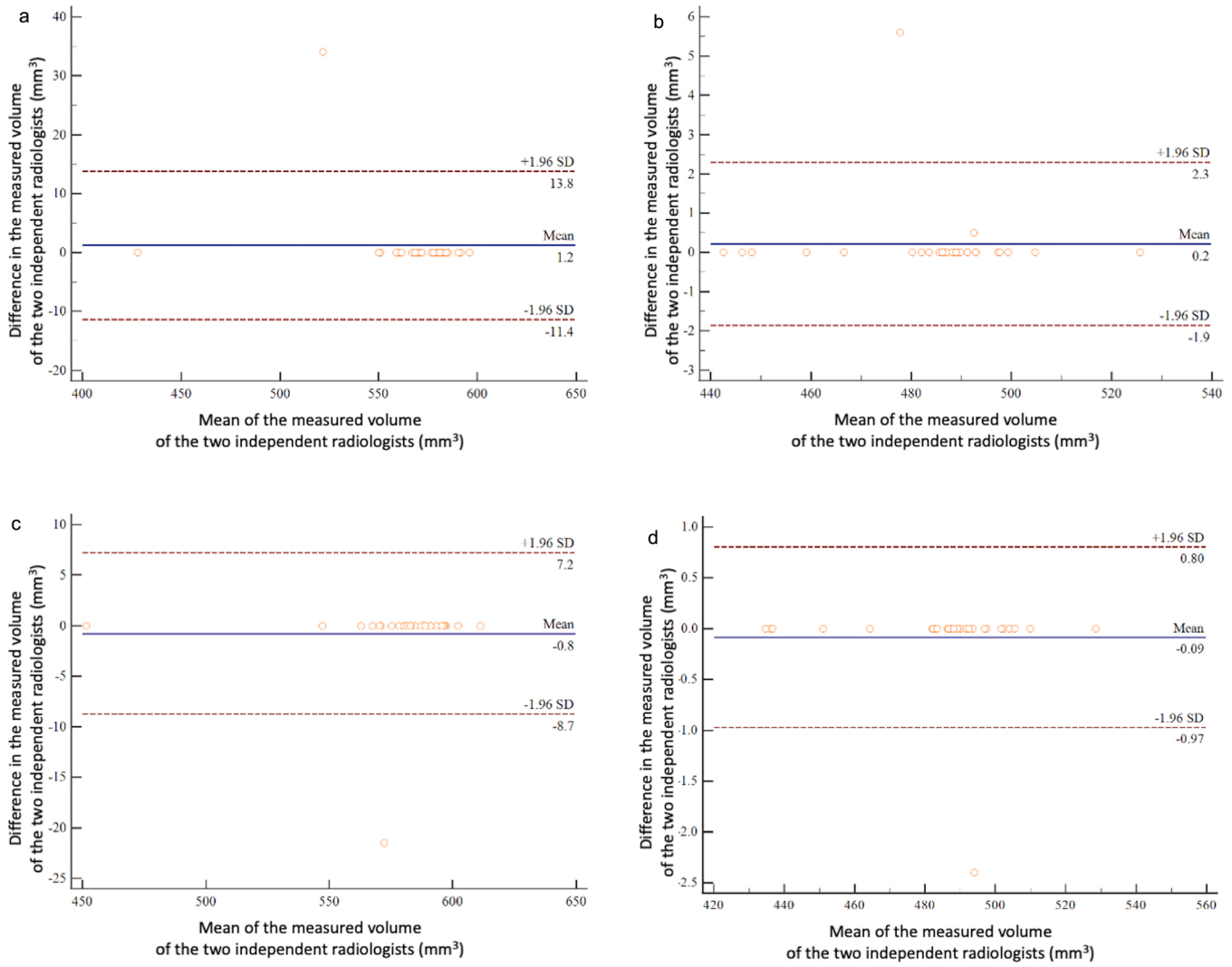

Fig. 3. Interobserver agreement regarding tumor volume in the phantom study. The Bland-Altman plots show the relative differences in tumor volumes between measurements by the two radiologists against the tumor volume. The horizontal axis of the graph shows the mean of the measured volumes of the two independent radiologists, and the vertical axis shows the difference in the measured volumes of them. The solid line indicates the mean difference (bias). Top and bottom dashed lines indicate upper and lower limits of agreement. (a) Bland-Altman plot of the measured volumes for the −800 HU nodule using the high-resolution setting in the phantom study. (b) Bland-Altman plot of the measured volumes of the −630 HU nodule using the high-resolution setting in the phantom study. (c) Bland-Altman plot of the measured volumes of the −800 HU nodule using the conventional setting in the phantom study. (d) Bland-Altman plot of the measured volumes of the −630 HU nodule using the conventional setting in the phantom study.

However, this is problematic if a voxel consists partly of lung parenchyma and partly of a nodule. Partial-volume voxels at the nodule margin can either be counted toward the nodule or excluded depending on the threshold set by the software, resulting in either over- or underestimation of the nodule volume. Goo et al. reported that thresholds of −500 and −400 HU resulted in smaller errors than those of −600 and −300 HU [13]. In our phantom study, the volume of the −800 HU nodule determined using the C-setting with its higher measurement error was larger than the assumed volume; hence, the measurement software we used tended to include these partial-volume voxels as a part of the nodule. Significant differences between the HR-setting and C-setting were only observed for the evaluation of the −800 HU artificial nodule. A previous study showed that volumetric measurement errors were increased when the nodule was fainter [6,14]. It was implicated that this was related to the reduced contrast between the GGN and the lung parenchyma [6]. We speculate that the HR-setting has the advantage of accurately delineating nodules by reducing partial volume effects when measuring the volume of the −800 HU nodule with its smaller differences in boundary attenuation between the normal lung parenchyma and nodules.

In clinical cases, GGNs with an average attenuation of about −740 HU did not have the same results as the −800 HU GGNs in the phantom study. This was probably because only one clinical nodule had CT attenuation values of −800 HU or lower. If the clinical nodules had been fainter such as the −800 HU artificial nodule, the results might have been similar to those in the phantom study. In addition, the artificial nodules used in the phantom study were simple spheres, but the nodules in the clinical study had irregular shapes and various sizes. Volumetric measurement by semi-automated software depends not only on attenuation but also on other factors, such as size and shape [13–15]. This difference in nodule shape and size might also have influenced the volumetry results. In clinical practice, there are various attenuation of GGNs. In the clinical study, there were significant differences between HR- and C-settings regarding minimum and maximum CT attenuation, although the mean attenuation and GGN mass were not affected. This might indicate shading differences and heterogeneity within nodules. The difference in maximum CT attenuation may affect the early detection and quantification of the solid component of GGNs; the clinical

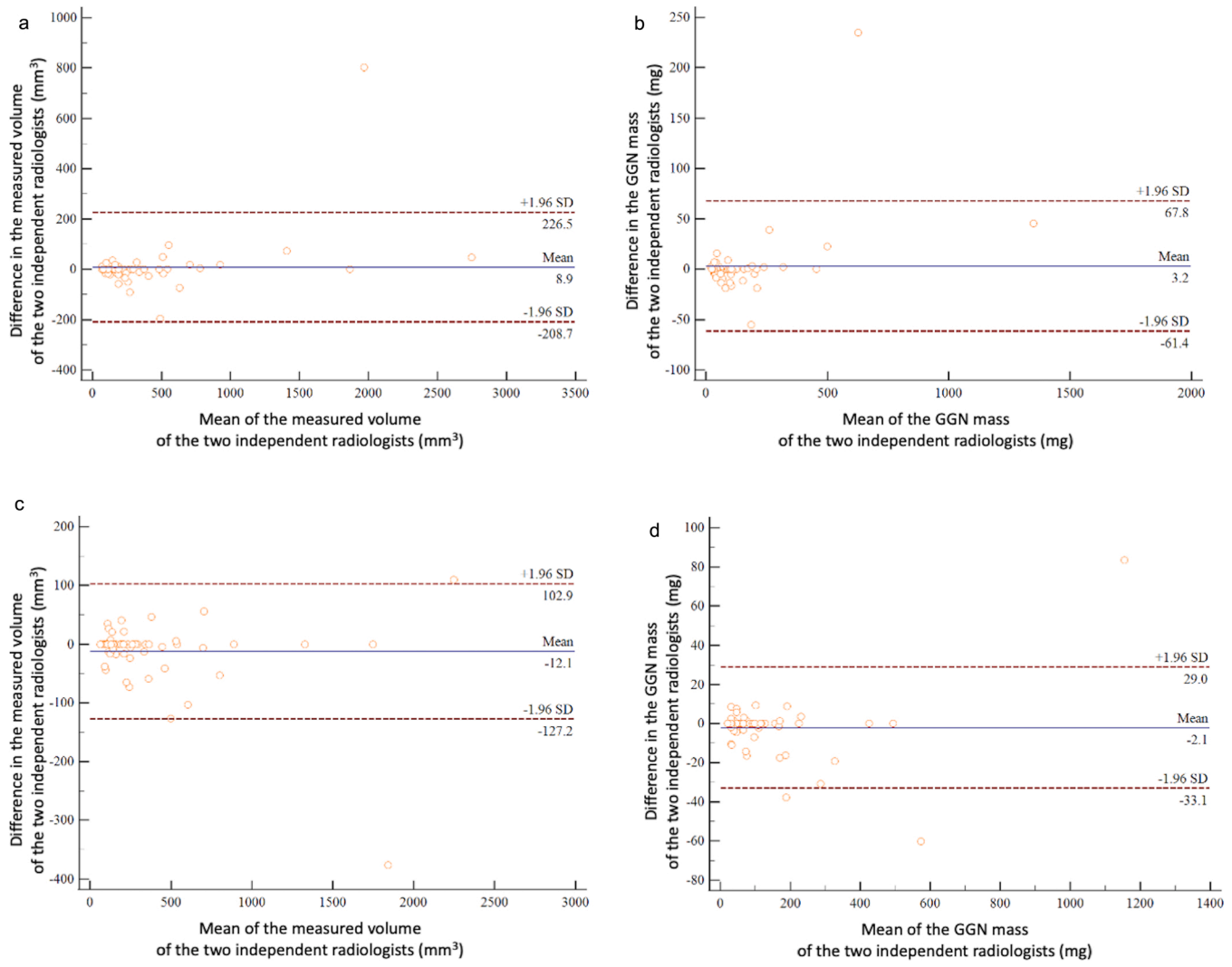

Fig. 4. Interobserver agreement regarding tumor volume and GGN mass in the clinical study. The Bland-Altman plots show the relative differences in tumor volumes between measurements by the two radiologists against the tumor volume and GGN mass. The horizontal axis of the graph shows the mean of the measured volumes or GGN mass of the two independent radiologists, and the vertical axis shows the difference in the measured volumes or GGN mass of them. The solid line indicates the mean difference (bias). Top and bottom dashed lines indicate upper and lower limits of agreement. (a) Bland-Altman plot of the measured volumes using the high-resolution setting in the clinical study. (b) Bland-Altman plot of GGN mass values using the high-resolution setting in the clinical study. (c) Bland-Altman plot of measured volumes using the conventional setting in the clinical study. (d) Bland-Altman plot of GGN mass values using the conventional setting in the clinical study.

significance of the difference in minimum CT attenuation is unclear. The development of new solid portions is considered a sign of GGN growth and malignancy [16]. Even if subsolid nodules have the same volume and mass in the two settings, the HR-setting may help to detect solid nodule components, which may facilitate the diagnosis and subsequent management of GGNs. We evaluated not only the volume but also the mass in GGNs. The latter parameter can detect GGN changes at an earlier stage than volume alone and can simultaneously quantify changes in nodule density and size [11]. However, in our study, significant differences in mass were the same as those in volume, and the superiority of the parameter GGN mass was not demonstrated.

The aggressiveness of GGNs can be estimated based on VDT measurements [3,4]. The size of GGNs, including atypical adenomatous hyperplasia, increases gradually and often does not change over months or years. Because the VDT of atypical adenomatous hyperplasia is very long, averaging 859.2 ± 428.9 days, it is very difficult to assess the growth rate visually on axial CT images [3]. Thus, volumetric measurements using the HR-setting with volumetry software might influence VDT calculations of GGNs. Software-aided volume measurements can be more accurate on HR-setting images, obtained with reduced slice thickness and larger matrix size. Volumetric measurements on HR-setting images might facilitate more accurate VDT assessments, which would help to estimate the aggressiveness of GGNs. Further studies with larger sample sizes are needed to validate VDT evaluations over time.

There are several limitations to this study. First, in clinical cases, we did not know the exact nodule volumes, because the maximum tumor volume on CT images and in resected lung cancer tissues cannot always be accurately compared, since lung specimens tend to collapse after resection. This may be of particular relevance to cases with GGNs on CT. Therefore, the possibility that the results of this study depended on the observer can not be denied. Second, we used only one type of software for 3D volumetry. Had we used another type of volumetry software, different results might have been obtained. Third, we compared two settings of the same CT scanner. Spatial resolution depends more heavily on the CT scanner itself than on reconstruction parameters. The difference might have been more pronounced if we compared two CT scanners, such as HSR-CT and C-CT scanners, rather than the reconstruction methods used with the same scanner. Fourth, we did not assess the noise. HSR-CT can provide higher image quality but generates more noise than

C-CT [17]. Thinner slices provide more accurate volume measurements, but thinner slices increase the noise [7]. Although noise may affect volume measurements of lung nodules, we speculate that the effect of noise on volume measurements is limited. Further investigations using a larger cohort are needed to validate our results.

In conclusion, significant differences in GGN volume were observed between the HR-setting and the C-setting for a phantom representing a −800 HU nodule, and the HR-setting influenced the detection of the maximum and minimum CT attenuation in GGNs. The improved detection of the maximum attenuation in the HR-setting might affect the early discovery of solid GGN components during follow up.

Ethical statement

This study was approved by the institutional ethics review board. The need to obtain informed consent for this retrospective review of patient records and images was waived.

Funding

This research did not receive any specific grant from funding agencies in the public, commercial, or not-for-profit sectors.

CRediT authorship contribution statement

Yuriko Yoshida: Conceptualization, Formal analysis, Investigation, Data curation, Writing - original draft, Visualization. **Masahiro Yanagawa:** Conceptualization, Formal analysis, Methodology, Data curation, Writing - review & editing, Supervision, Project administration. **Akinori Hata:** Conceptualization, Methodology, Writing - review & editing. **Yukihisa Sato:** Validation, Investigation. **Mitsuko Tsubamoto:** Validation, Investigation. **Shuhei Doi:** Investigation. **Kazuki Yamagata:** Investigation. **Tomo Miyata:** Investigation. **Noriko Kikuchi:** Investigation. **Noriyuki Tomiyama:** Supervision, Project administration.

Declaration of Competing Interest

There are no conflicts of interest to declare.

References

[1] C.M. Park, J.M. Goo, H.J. Lee, C.H. Lee, E.J. Chun, J.G. Im, Nodular ground-glass opacity at thin-section CT: histologic correlation and evaluation of change at follow-up, Radiographics 27 (2007) 391–408, https://doi.org/10.1148/rg.272065061.

[2] C.I. Henschke, D.F. Yankelevitz, R. Mirtcheva, G. McGuinness, D. McCauley, O. S. Miettinen, E.L.C.A.P. Group, CT screening for lung cancer: frequency and significance of part-solid and nonsolid nodules, AJR Am. J. Roentgenol. 178 (2002) 1053–1057, https://doi.org/10.2214/ajr.178.5.1781053.

[3] S. Oda, K. Awai, K. Murao, A. Ozawa, D. Utsunomiya, Y. Yanaga, K. Kawanaka, Y. Yamashita, Volume-doubling time of pulmonary nodules with ground glass opacity at multidetector CT: assessment with computer-aided three-dimensional volumetry, Acad. Radiol. 18 (2011) 63–69, https://doi.org/10.1016/j.acra.2010.08.022.

[4] A. Borghesi, D. Farina, S. Michelini, M. Ferrari, D. Benetti, S. Fisogni, A. Tironi, R. Maroldi, Pulmonary adenocarcinomas presenting as ground-glass opacities on multidetector CT: three-dimensional computer-assisted analysis of growth pattern and doubling time, Diagn. Interv. Radiol. 22 (2016) 525–533, https://doi.org/10.5152/dir.2016.16110.

[5] D. Han, M.A. Heuvelmans, M. Oudkerk, Volume versus diameter assessment of small pulmonary nodules in CT lung cancer screening, Transl. Lung Cancer Res. 6 (2017) 52–61, https://doi.org/10.21037/tlcr.2017.01.05.

[6] J.P. Ko, H. Rusinek, E.L. Jacobs, J.S. Babb, M. Betke, G. McGuinness, D.P. Naidich, Small pulmonary nodules: volume measurement at chest CT—phantom study, Radiology 228 (2003) 864–870, https://doi.org/10.1148/radiol.2283020059.

[7] M. Yanagawa, A. Hata, O. Honda, N. Kikuchi, T. Miyata, A. Uranishi, S. Tsukagoshi, N. Tomiyama, Subjective and objective comparisons of image quality between ultra-high-resolution CT and conventional area detector CT in phantoms and cadaveric human lungs, Eur. Radiol. 28 (2018) 5060–5068, https://doi.org/10.1007/s00330-018-5491-2.

[8] H. MacMahon, D.P. Naidich, J.M. Goo, K.S. Lee, A.N.C. Leung, J.R. Mayo, A. C. Mehta, Y. Ohno, C.A. Powell, M. Prokop, G.D. Rubin, C.M. Schaefer-Prokop, W. D. Travis, P.E. Van Schil, A.A. Bankier, Guidelines for management of incidental pulmonary nodules detected on CT images: from the Fleischner Society 2017, Radiology 284 (2017) 228–243, https://doi.org/10.1148/radiol.2017161659.

[9] J.M. Bland, D.G. Altman, Measuring agreement in method comparison studies, Stat. Methods Med. Res. 8 (1999) 135–160, https://doi.org/10.1177/096228029900800204.

[10] R.T. Mull, Mass estimates by computed tomography: physical density from CT numbers, AJR Am. J. Roentgenol. 143 (1984) 1101–1104, https://doi.org/10.2214/ajr.143.5.1101.

[11] B. de Hoop, H.A. Gietema, S. van de Vorst, K. Murphy, R.J. van Klaveren, M. Prokop, Pulmonary ground-glass nodules: increase in mass as an early indicator of growth, Radiology 255 (2010) 199–206, https://doi.org/10.1148/radiol.09090571.

[12] H.T. Winer-Muram, S.G. Jennings, C.A. Meyer, Y. Liang, A.M. Aisen, R.D. Tarver, R.C. McGarry, Effect of varying CT section width on volumetric measurement of lung tumors and application of compensatory equations, Radiology 229 (2003) 184–194, https://doi.org/10.1148/radiol.2291020859.

[13] J.M. Goo, T. Tongdee, R. Tongdee, K. Yeo, C.F. Hildebolt, K.T. Bae, Volumetric measurement of synthetic lung nodules with multi–detector row CT: effect of various image reconstruction parameters and segmentation thresholds on measurement accuracy, Radiology 235 (2005) 850–856, https://doi.org/10.1148/radiol.2353040737.

[14] E.T. Scholten, C. Jacobs, B. van Ginneken, M.J. Willemink, J.M. Kuhnigk, P.M. van Ooijen, M. Oudkerk, W.P. Mali, P.A. de Jong, Computer-aided segmentation and volumetry of artificial ground-glass nodules at chest CT, AJR Am. J. Roentgenol. 201 (2013) 295–300, https://doi.org/10.2214/AJR.12.9640.

[15] X. Xie, M.J. Willemink, P.A. de Jong, P.M. an Ooijen, M. Oudkerk, R. Vliegenthart, M.J. Greuter, Small irregular pulmonary nodules in low-dose CT: observer detection sensitivity and volumetry accuracy, AJR Am. J. Roentgenol. 202 (2014) W202–W209, https://doi.org/10.2214/AJR.13.10830.

[16] H.W. Lee, K.N. Jin, J.K. Lee, D.K. Kim, H.S. Chung, E.Y. Heo, S.H. Choi, Long-term follow-up of ground-glass nodules after 5 years of stability, J. Thorac. Oncol. 14 (2019) 1370–1377, https://doi.org/10.1016/j.jtho.2019.05.005.

[17] R. Kakinuma, N. Moriyama, Y. Muramatsu, S. Gomi, M. Suzuki, H. Nagasawa, M. Kusumoto, T. Aso, Y. Muramatsu, T. Tsuchida, K. Tsuta, A.M. Maeshima, N. Tochigi, S. Watanabe, N. Sugihara, S. Tsukagoshi, Y. Saito, M. Kazama, K. Ashizawa, K. Awai, O. Honda, H. Ishikawa, N. Koizumi, D. Komoto, H. Moriya, S. Oda, Y. Oshiro, M. Yanagawa, N. Tomiyama, H. Asamura, Ultra-high-resolution computed tomography of the lung: image quality of a prototype scanner, PLoS One 10 (2015), e0137165, https://doi.org/10.1371/journal.pone.0137165.